

## Pressure Induced Structural and Electronic Bandgap properties of Anatase and Rutile $\text{TiO}_2$

(Struktur dan Ciri Jurang Jalur Elektronik Anatas dan  $\text{TiO}_2$  Rutil yang dirangsang oleh Tekanan)

TARIQ MAHMOOD\*, CHUANBAO CAO, RASHID AHMED, MAQSOOD AHMED, M.A. SAEED,  
ABRAR AHMED ZAFAR, TALAB HUSAIN & M.A. KAMRAN

### ABSTRACT

In this study, we present the structural and electronic bandgap properties of anatase and rutile titanium dioxide by applying ultrasoft pseudo-potential plane wave approach developed within the frame of density functional theory (DFT). We used generalized gradient approximation (GGA) proposed by Perdew-Burke-Ernzerhof (PBE) for exchange correlation potential. In our pressure driven investigations, geometry optimization is carried out for different values of pressure over a range of 0-100 GPa and subsequently related structural parameters and bandgap values of anatase and rutile titanium dioxide ( $\text{TiO}_2$ ) have been calculated. In both cases, the lattice constants ( $a, c$ ) and volume decreased as the pressure was increased. Similarly, internal parameter for anatase increased and for rutile  $\text{TiO}_2$  it decreased under high pressure. The value of  $c/a$  decreased for anatase and increased for rutile  $\text{TiO}_2$  as a function of pressure. Our band structure analysis showed different behavior of bandgap between anatase and rutile  $\text{TiO}_2$ . The conduction band of anatase  $\text{TiO}_2$  moved opposite to the conduction band of rutile  $\text{TiO}_2$  as we increased the pressure. Additionally we used the Birch-Murnaghan equation of state to obtain the equilibrium volume ( $V_0$ ), bulk modulus ( $B_0$ ) and pressure derivative of bulk modulus ( $B'_0$ ) at zero pressure. The calculated results are in good agreement with previous experimental as well as theoretical results.

**Keywords:** Conduction band; density function theory; pressure

### ABSTRAK

Di dalam kajian ini, kami membentangkan ciri struktur dan jurang jalur elektronik bagi anatas dan titanium dioksida rutil dengan menggunakan pendekatan gelombang satah pseudo-keupayaan ultralembut yang dibangunkan dalam kerangka teori fungsi ketumpatan (DFT). Kami menggunakan penganggaran cerun umum (GGA) yang diusulkan oleh Perdew-Burke-Ernzerhof (PBE) untuk keupayaan korelasi pertukaran. Kajian tekanan yang didorong pengoptimuman geometri telah dijalankan untuk nilai tekanan yang berbeza pada julat 0-100 GPa. Parameter struktur dan nilai jurang jalur anatas dan titanium dioksida rutil telah dikira. Dalam kedua-dua kes, nilai pemalar kekisi ( $a, c$ ) dan isi padu menurun apabila tekanan meningkat. Parameter dalaman untuk anatas meningkat dan untuk  $\text{TiO}_2$  rutil menurun pada tekanan tinggi. Nilai  $c/a$  menurun untuk anatas dan meningkat untuk  $\text{TiO}_2$  rutil sebagai fungsi tekanan. Analisis struktur jalur menunjukkan tingkah laku yang berbeza antara jurang jalur anatas dan  $\text{TiO}_2$  rutil. Jalur konduksi anatas  $\text{TiO}_2$  bergerak dengan berlawanan arah terhadap jalur konduksi  $\text{TiO}_2$  rutil apabila tekanan meningkat. Persamaan keadaan Birch-Murnaghan telah digunakan untuk mendapatkan isi padu keseimbangan ( $V_0$ ) modulus pukal ( $B_0$ ) dan terbitan tekanan modulus pukal ( $B'_0$ ) pada tekanan sifar. Keputusan yang diperoleh adalah selari dengan keputusan uji kaji dan teori yang sebelumnya.

**Kata kunci:** Jalur konduksi; tekanan; teori fungsi ketumpatan

### INTRODUCTION

Titanium dioxide ( $\text{TiO}_2$ ) is one of the most complex transition metal oxides, which readily exists and well described experimentally with a broad range of applications (Diebold 2003).  $\text{TiO}_2$  has a versatile range of industrial applications such as photo-electrode (Griffin & Siefering 1990), electronics (Wu & Chen 1990), gas-sensing, painting (Varghese & Grimes 2003) and dye-sensitized solar cells (Lazzeri et al. 2001). Due to the versatile range of industrial applications, long term chemical steadiness, marvelous photocatalytic activity and photoelectrochemical hydrogen production through water

splitting,  $\text{TiO}_2$  is under intense study for a long time (Asahi et al. 2001; Diwald et al. 2004; Fujishima & Honda 1972; Gole et al. 2004; Irie et al. 2003; Lindgren et al. 2003; Nakamura et al. 2004; Sakthivel & Kisch 2003).

In the literature, different phases have been discussed of this potential material but rutile and anatase phases have been most frequently investigated for the large bandgap 3.2 eV for anatase (Baizaee & Mousavi 2009) and 3.0 eV for rutile (Burdett et al. 1987) semiconductors. Although many investigations are being performed to make  $\text{TiO}_2$  visible light absorbing material by doping Fe, Mo, Cr, Co, C and N (Di Valentin et al. 2004, 2005; Khan et al. 2002;

Zhao et al. 2004) or introducing oxygen vacancies (Lin et al. 2005), in the current era of science and technology, the wide bandgap materials such as  $\text{TiO}_2$  is under consideration for potential applications such as ferroelectric material at low pressures (Liu et al. 2009), electronic devices (Wu & Chen 1990), fabrication of antireflection coatings, optical wave guides (Griffin & Siefering 1990) and realization of spintronic devices (Carp et al. 2004; Diebold 2003; Janisch et al. 2005).

Structural parameters and bandgap value of anatase and rutile titanium dioxide have been reported in some previous theoretical researches (Cho et al 2006; Fox et al. 2010; Islam et al. 2007; Labat et al. 2007; Mattioli et al 2008; Persson & Da Silva 2005; Shirley et al. 2010), employing different methods (Pseudopotential Hartree-Fock (PHF), Orthogonalized linear combination of atomic orbitals (OLCAO), full-potential linearized augmented plane-wave (FP-LAPW)). To the best of our knowledge there is no theoretical study on the structural and electronic bandgap calculations for anatase and rutile  $\text{TiO}_2$  under hydrostatic pressure.

In this work we present investigations about the structural and electronic bandgap of anatase and rutile titanium dioxide under different values of hydrostatic pressure, using first-principles plane-wave ultrasoft pseudo-potential method. The details of computational method are given in the following section followed by results and discussion. The last section represents the conclusion of this work.

#### COMPUTATIONAL DETAILS

$\text{TiO}_2$ -anatase lies in the tetragonal crystal system; I41/AMD space group (number 141) and  $\text{TiO}_2$ -rutile also belongs to the same crystal system; P42/mnm space group

(number 136). This investigation was performed using first-principles plane-wave ultra-soft pseudo-potential method within CASTEP code (Segall et al. 2002). The generalized gradient approximation (GGA) is used as an exchange-correlation function proposed by Perdew-Burke-Ernzerhof (PBE) (Perdew et al. 1996). Pseudo atomic calculation performed for Ti:  $3s^23p^63d^24s^2$  and O:  $2s^22p^4$ , respectively. We choose the cutoff energy 300 eV to expand the electronic wave functions in plane waves and  $k$  point set  $4\times4\times4$  under the Monkhorst-Pack scheme (Monkhorst & Pack 1976) for both anatase and rutile  $\text{TiO}_2$ .

The Pulay density mixed method was used to calculate the ground state energy which was set to  $2\times10^{-6}\text{eV atom}^{-1}$ . The Broyden and Goldfarb (BFGS) method (Fische & Almlöf 1992) was used to optimize the geometry of anatase and rutile  $\text{TiO}_2$ .

#### RESULTS AND DISCUSSION

We present the structural and bandgap studies of anatase and rutile  $\text{TiO}_2$  under stress. In order to get the best results, we carried out the prescribed calculation of the anatase and rutile structure using GGA-PBE comprehensively. For this purpose we used the experimental values of lattice constants for anatase ( $a=b=3.782\text{\AA}$ ,  $c=9.502\text{\AA}$ ) and rutile ( $a=b=4.586\text{\AA}$ ,  $c=2.954\text{\AA}$ )  $\text{TiO}_2$  (Burkett et al. 1987) and optimized the structures, respectively. The optimized lattice parameters and obtained bandgaps values for anatase and rutile  $\text{TiO}_2$  from our GGA-PBE calculations are presented in Table 1. From Table 1, it is obvious that our obtained structural parameters for both anatase and rutile  $\text{TiO}_2$  are in very good agreement with the experimental values (Burkett et al. 1987). Our calculated structural parameters ( $a=b=3.798\text{\AA}$ ,  $c=9.852\text{\AA}$ ,  $u=0.206$ , equatorial bond length

TABLE 1. Optimized structural parameters for anatase and rutile  $\text{TiO}_2$  compared with experiment and other theoretical results

	Exp. (Burkett et al. 1987; Tang et al. 1993)	This work	FLAPW-LDA (Asahi et al. 2000)	FP-LAPW (Chen et al. 2004)	GGA-PW91 (Yin et al. 2010)
<b>Anatase</b>					
$a$	3.782	3.798	3.692	3.823	3.8188
$c$	9.502	9.852	9.471	9.612	9.6875
$u$	0.208	0.206	0.206	0.208	0.2069
$d_{eq}\text{(\AA)}$	1.932	1.948	1.893	1.954	1.95
$d_{ap}\text{(\AA)}$	1.979	2.013	1.948	1.995	2.00
$2\theta^\circ$	156.3°	154.234°	154.4°	155.92°	---
$E_g\text{(eV)}$	3.2	2.179	2.0	2.13	1.88
Exp. (Burkett et al. 1987; Pascual et al. 1978)					
		This work	GGA-PW91 (Yin et al. 2010)	GGA-PW91 (Ma et al. 2009)	TDDFT (Thilagam et al. 2011)
<b>Rutile</b>					
$a$	4.586	4.705	4.656	4.630	4.590
$c$	2.954	2.966	2.967	2.957	2.960
$u$	0.305	0.308	0.3046	---	---
$d_{eq}\text{(\AA)}$	1.946	1.956	1.96	1.955	---
$d_{ap}\text{(\AA)}$	1.976	2.052	2.01	2.047	1.945(avg)
$2\theta^\circ$	98.8°	98.634°	---	---	---
$E_g\text{(eV)}$	3.0	1.969	1.64		2.01

$(\text{Ti}-\text{O}) d_{eq} = 1.948 \text{ \AA}$ , apical bond length  $(\text{Ti}-\text{O}) d_{ap} = 2.013 \text{ \AA}$  and angle  $(\text{Ti}-\text{O}-\text{Ti}) 2\theta = 154.234^\circ$  and bandgap ( $E_g = 2.179 \text{ eV}$ ) for anatase  $\text{TiO}_2$  are better than previous theoretical results (Asahi et al. 2000; Chen & Cao 2004; Yin et al. 2010) and in consistent with experimental values ( $a=b=3.782 \text{ \AA}$ ,  $c=9.502 \text{ \AA}$ ,  $u=0.208$ ,  $d_{eq} = 1.932 \text{ \AA}$ ,  $d_{ap} = 1.979 \text{ \AA}$ ,  $2\theta = 156.3^\circ$  and  $E_g = 3.2 \text{ eV}$ ) (Burdett et al. 1987; Tang et al. 1993). Furthermore, it can be seen from Table 1 that the values of structural parameters ( $a=b=4.705 \text{ \AA}$ ,  $c=2.966 \text{ \AA}$ ,  $u=0.308$ ,  $d_{eq} = 1.956 \text{ \AA}$ ,  $d_{ap} = 2.052 \text{ \AA}$  and  $2\theta = 98.634^\circ$ ) and bandgap ( $E_g = 1.696 \text{ eV}$ ) for rutile  $\text{TiO}_2$  are also better than the listed computational results (Ma et al. 2009; Thilagam et al. 2011; Yin et al. 2010) and comparable with experimental results ( $a=b=4.586 \text{ \AA}$ ,  $c=2.954 \text{ \AA}$ ,  $u=0.305$ ,  $d_{eq} = 1.946 \text{ \AA}$ ,  $d_{ap} = 1.976 \text{ \AA}$ ,  $2\theta = 156.3^\circ$  and  $E_g = 3.0 \text{ eV}$ ) (Burdett et al. 1987; Pascual et al. 1978).

The structural parameters (lattice constants ( $a, c$ ),  $c/a$  ratio, internal parameter ( $u$ ) and volume ( $V$ )) of anatase and rutile  $\text{TiO}_2$  at different hydrostatic pressures are shown in Figures 1(a) to 1(d). Figures 1(a) and 1(d) are plots of the lattice constants ( $a, c$ ) and volume  $V$  as a function of pressure. From these plots (Figures 1(a) & 1(d)), it can be seen that the values of lattice constants and volume are decreasing as pressure is increasing in both cases (anatase and rutile  $\text{TiO}_2$ ).

The graphs of the  $c/a$  ratio and internal parameter as functions of pressure are shown in Figures 1(b) and 1(c),

the  $c/a$  ratio reducing for anatase  $\text{TiO}_2$  and increasing for rutile  $\text{TiO}_2$  as the pressure is increased. The internal parameter (Figure 1(c)) increases in the case of anatase structure and decreases for rutile structure at higher pressure. Interestingly, the crystal structures are stable over entire range of pressure from 0-100 GPa for both anatase and rutile  $\text{TiO}_2$ . We have checked the symmetry after optimization step at each pressure value (0-100 GPa) by using *find-symmetry* tool as incorporated within material studio 5.0 version. Furthermore, in order to obtain the equilibrium volume ( $V_0$ ), bulk modulus ( $B_0$ ) and pressure derivative of bulk modulus ( $B'_0$ ) for anatase and rutile structure we used the Birch Murnaghan equation of state (Murnaghan 1944).

Table 2 summarizes our calculated results on the equation of state parameters of the anatase and rutile  $\text{TiO}_2$  at zero pressure. Here, the obtained value of zero-pressure volume ( $142.15 \text{ \AA}^3$ ) for anatase  $\text{TiO}_2$  is slightly overestimated as compared with experimental value ( $136.278$ ) (Arlt et al. 2000) and other DFT based values (Iuga et al. 2007; Yin et al. 2010) but is in good agreement with theoretical value (Arlt et al. 2000). Moreover, the obtained value of bulk modulus ( $188 \text{ GPa}$ ) of anatase structure is in consistent with experiment ( $179 \text{ GPa}$ ) (Arlt et al. 2000) as compared with reported computational results (Arlt et al. 2000; Iuga et al. 2007; Yin et al. 2010). Also, the calculated result of pressure derivative of bulk

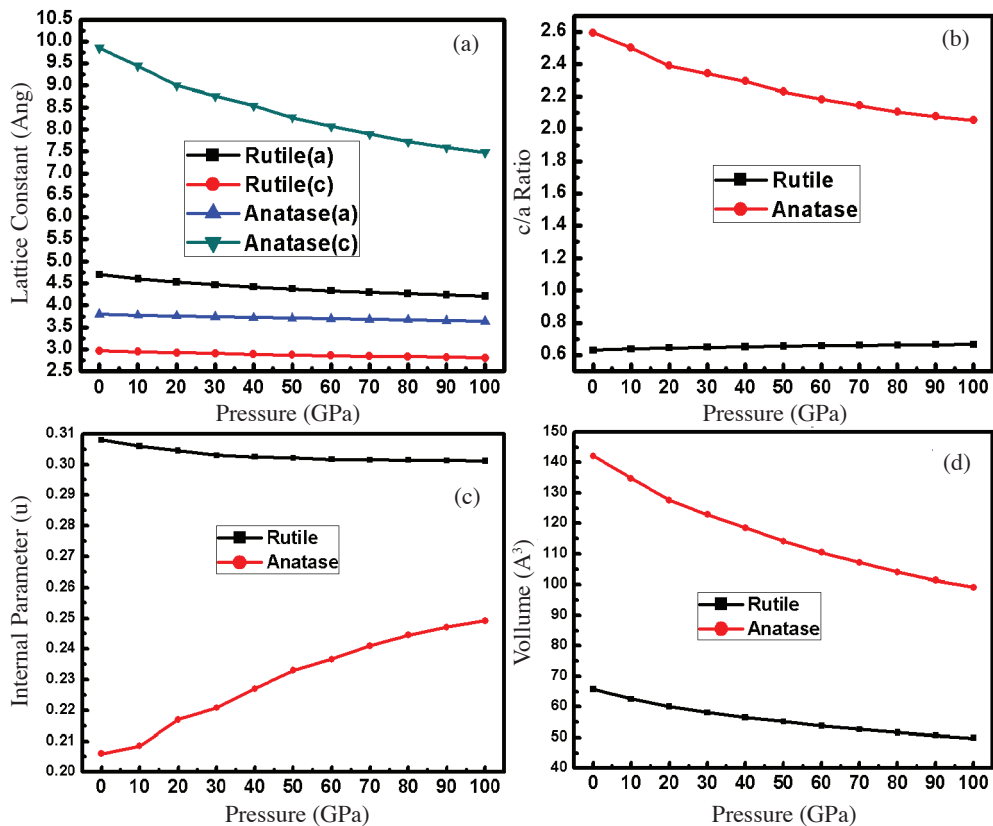


FIGURE 1. Calculated lattice parameters: (a)  $a, c$ , (b) the axial ratio  $c/a$ , (c) internal parameter ( $u$ ) and (d) the unit cell volume ( $V$ ) as function of pressure (GPa)

TABLE 2. Calculated equilibrium volume ( $V_0$ ), bulk modulus ( $B_0$ ) and pressure derivative of bulk modulus ( $B'_0$ ) for anatase and rutile  $\text{TiO}_2$  at zero pressure compared with experiment and other theoretical results

	Exp. (Arlt et al. 2000)	This work	GGA-PBE (Iuga et al. 2007)	aiPI (Arlt et al. 2000)	GGA-PW91 (Yin et al. 2010)
<b>Anatase</b>					
$V_0$ ( $\text{\AA}^3$ )	136.278	142.15	138.3	143.8	134.56
$B_0$ (GPa)	179	188	221	189.5	146
$B'_0$	4.5	3.7	4.0	3.42	4
	Exp. (Arlt et al. 2000)	This work	VASP-GGA (Zhou et al. 2010)	CRYSTAL-GGA (Swamy et al. 2007)	PAW-LDA (Yahya Al-Khatabeh et al. 2009)
<b>Rutile</b>					
$V_0$ ( $\text{\AA}^3$ )	62.44	65.67	64.34	63.78	61
$B_0$ (GPa)	211	244	221	215	250
$B'_0$	6.5	3.6	4.8	5.35	4

modulus ( $B'_0 = 3.7$ ) has good agreement with experiment (Arlt et al. 2000) as well as theoretical results (Arlt et al. 2000; Iuga et al. 2007; Yin et al. 2010). In the case of rutile  $\text{TiO}_2$ , the obtained values of zero-pressure volume (65.67  $\text{\AA}^3$ ) and bulk modulus (244 GPa) are slightly higher than experiment (Arlt et al. 2000) and previous theoretical results (Swamy & Muddle 2007; Yahya Al-Khatabeh et al. 2009; Zhou et al. 2010). The lower value 3.6 of the  $B'_0$  for rutile  $\text{TiO}_2$  is obtained due to the overestimation of the equilibrium volume and bulk modulus in the total energy calculations.

From Figure 2 which is the graphical representation of bandstructure, it can be seen that the nature of bandgap is indirect. It can also be seen from Figure 2 (0-40 GPa), the maximum of valence band lies at the right side of the M-symmetry point and minimum of conduction band is on G-point. From Figure 2 (50-100 GPa), the maximum of valence band lies at M-point and minimum of conduction band remain the same on G-point. Furthermore, from the calculated bandstructure it is clear that the conduction band of anatase  $\text{TiO}_2$  shifts down as a function of pressure (equivalent to hydrostatic pressure) and maximum of valance band shifts towards left side. The bandgap ( $E_g$ ) reduces for anatase  $\text{TiO}_2$  as the pressure is increased. This is due to the decrease of lattice constants (Figure 1(a)),  $c/a$  ratio (Figure 1(b)) and volume (Figure 1(d)) and increase of internal parameter (Figure 1(c)) as a function of pressure. With the increase of pressure, the p states of Ti and O are delocalized, which result in the shifting of valance band maximum to higher energy levels and conduction band minimum to lower energy levels, which ultimately reduces the badgap of anatase  $\text{TiO}_2$  (Shi et al. 2009).

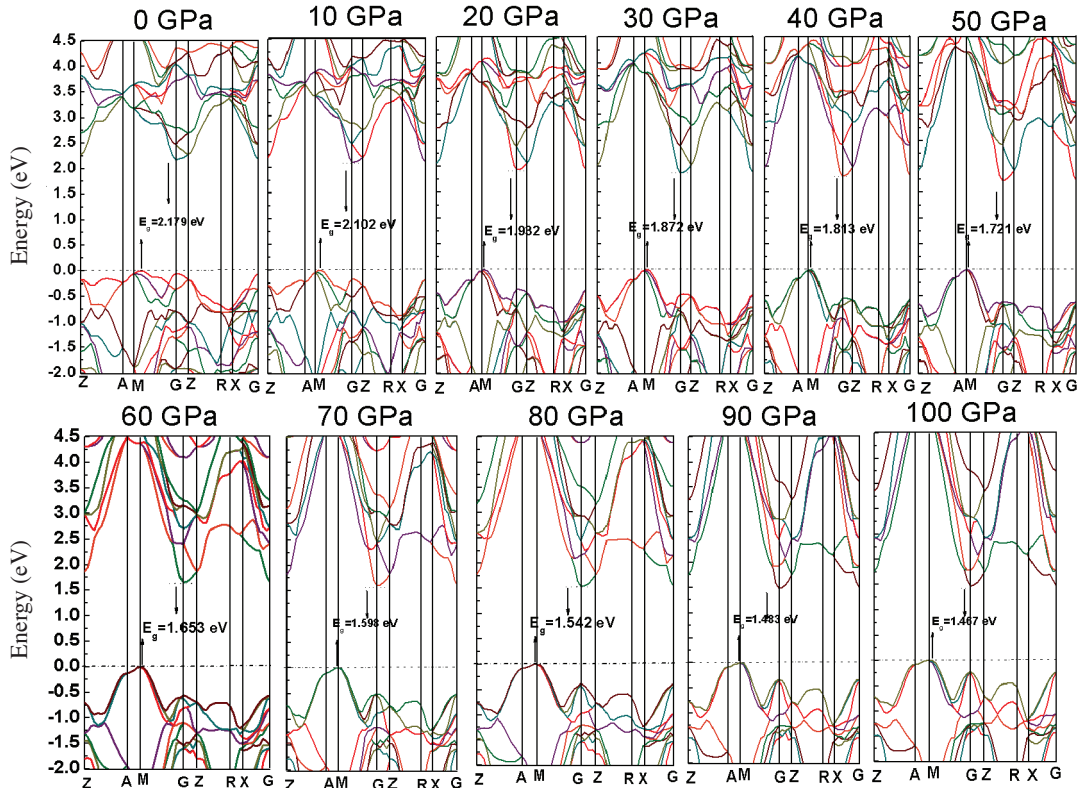
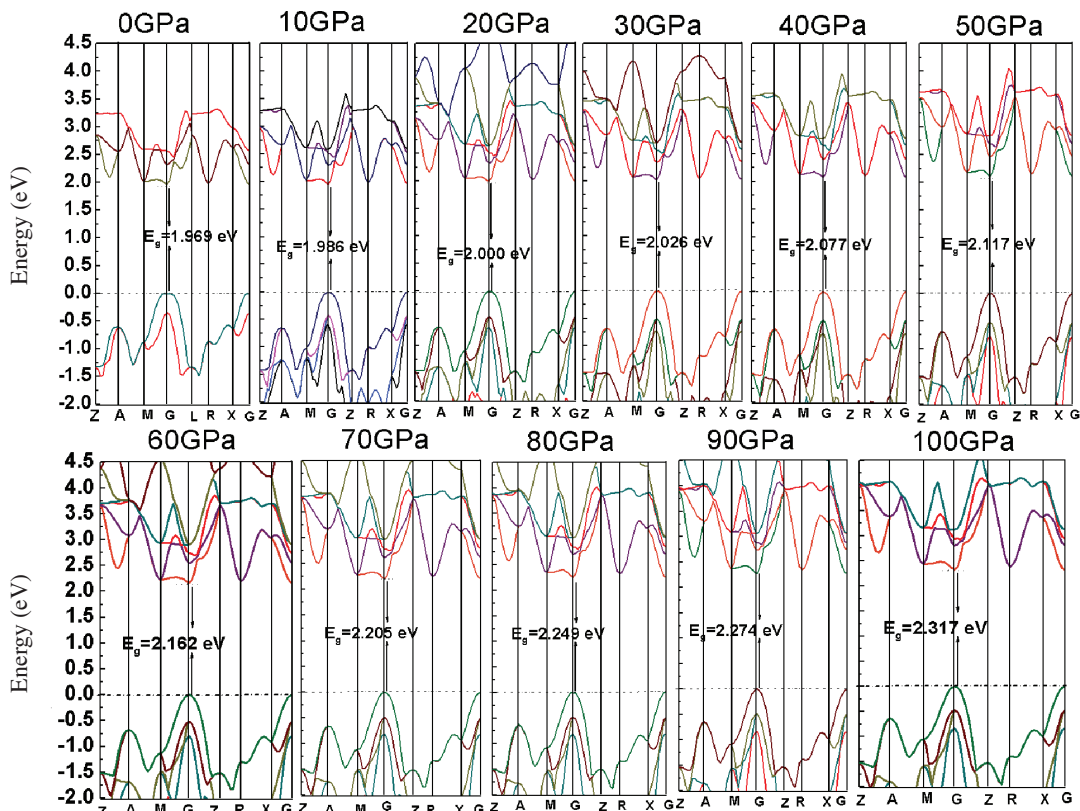
Figure 3 is the graphical representation of bandstructure of rutile  $\text{TiO}_2$ , which exhibit its direct bandgap nature. From Figure 3 (0-100 GPa), the maximum of valance band lies at the symmetry point G and minimum of conduction band is on G-point. Figure 3 (0 GPa) shows that the maximum of valance band is in flat

shape but Figure 3 (10-100 GPa) are representing that the edge of the maximum of valance band becoming sharp. Furthermore, our calculations show that the conduction band of rutile  $\text{TiO}_2$  shifts up and maximum of valence band becomes sharp as pressure is increased.

The bandgap ( $E_g$ ) increased for rutile  $\text{TiO}_2$  as the pressure is increased. This is due to the fact that increasing the pressure, results in delocalization of  $d$  and  $p$  states of Ti and  $p$  states of O. This delocalization further results in shifting of valance band maximum to lower energy levels and conduction band minimum to higher energy levels and hence the bandgap is increased as observed by Shi et al. (2009) and Tariq et al. (2012).

## CONCLUSION

We have performed the structural and bandgap calculations of anatase and rutile  $\text{TiO}_2$ , using the generalized gradient approximation (GGA) for exchange correlation potential proposed by Perdew-Burke-Ernzerhof (PBE). Our calculated structural parameters ( $a$ ,  $c$ ,  $u$ ,  $d_{eq}$ ,  $d_{ap}$ ,  $2\theta$ ) bandgap ( $E_g$ ) and parameters of equation of state at zero pressure for both polymorphs (anatase and rutile  $\text{TiO}_2$ ) are consistent with the experiment. It can be seen from Figures 1(a) and 1(d) that the lattice parameters ( $a$ ,  $c$ ) and both volume decreased for anatase and rutile  $\text{TiO}_2$  with the rise of pressure. It is also found that, as pressure increases, the  $c/a$  ratio increases for rutile and decreases for anatase  $\text{TiO}_2$ . Similarly, the internal parameters increased for anatase and decrease for rutile  $\text{TiO}_2$  as pressure increased. The effect of pressure on bandgap for anatase and rutile phases also investigated. The bandgap decreased for anatase and increases for rutile  $\text{TiO}_2$  as pressure is increased. The results showed that the anatase and rutile  $\text{TiO}_2$  exhibit no phase transformation under high pressures (0-100 GPa) and room temperature. So we conclude that the anatase and rutile phases are stable at room temperature and high pressures up to 100 GPa.

FIGURE 2. Pressure induced band structures of anatase  $\text{TiO}_2$ FIGURE 3. Pressure induced band structures of rutile  $\text{TiO}_2$

## ACKNOWLEDGEMENT

This work was supported by National Natural Science Foundation of China (20471007, 50972017) and the Research Fund for the Doctoral Program of Higher Education of China (20101101110026). Two of the authors (Rashid Ahmed and M. Alam Saeed) would like to thank for the partial financial support of the Ministry of Higher Education (MOHE) Malaysia and Universiti Teknologi Malaysia (UTM) for this research work through grant no. Q. J13000.7126.00J33.

## REFERENCES

- Arlt, T., Bermejo, M., Blanco, M.A., Gerward, L., Jiang, J.Z., Staun Olsen, J. & Recio, J.M. 2000. High-pressure polymorphs of anatase  $\text{TiO}_2$ . *Phys. Rev. B* 61(21): 14414-14419.
- Asahi, R., Taga, Y., Mannstadt, W. & Freeman, A.J. 2000. Electronic and optical properties of anatase  $\text{TiO}_2$ . *Phys. Rev. B* 61(11): 7459-7465.
- Asahi, R., Morikawa, T., Ohwaki, T., Aoki, K. & Taga, Y. 2001. Visible-light photocatalysis in nitrogen-doped titanium oxides. *Science* 293: 269-271.
- Baizaei, S.M. & Mousavi, N. 2009. First-principles study of the electronic and optical properties of rutile  $\text{TiO}_2$ . *Physica B* 404: 2111-2116.
- Burdett, J.K., Hughbanks, T., Miller, G.J., Richardson, J.W. Jr. & Smith, J.V. 1987. Structural-electronic relationships in inorganic solids: Powder neutron diffraction studies of the rutile and anatase polymorphs of titanium dioxide at 15 and 295 K. *J. Am. Chem. Soc.* 109(12): 3639-3646.
- Carp, O., Huisman, C.L. & Reller, A. 2004. Photoinduced reactivity of titanium dioxide. *Prog. Solid State Chem.* 32(1-2): 33-177.
- Chen, Q. & Cao, H-H. 2004. *Ab initio* calculations of electronic structure of anatase  $\text{TiO}_2$ . *Chinese Physics B* 13(12): 2121.
- Cho, E., Han, S., Ahn, H-S., Lee, K-R., Kim, S.K. & Hwang, C.S. 2006. First-principles study of point defects in rutile  $\text{TiO}_{2-x}$ . *Phys. Rev. B* 73(19): 193202.
- Di Valentin, C., Pacchioni, G. & Selloni, A. 2004. Origin of the different photoactivity of n-doped anatase and rutile  $\text{TiO}_2$ . *Phys. Rev. B* 70(8): 085116.
- Di Valentin, C., Pacchioni, G., Selloni, A., Livraghi, S. & Giamello, E. 2005. Characterization of paramagnetic species in n-doped  $\text{TiO}_2$  powders by EPR spectroscopy and DFT calculations. *J. Phys. Chem. B* 109: 11414-11419.
- Diebold, U. 2003. The surface science of titanium dioxide. *Surf. Sci. Rep.* 48(5-8): 53-229.
- Diwald, O., Thomphson, T.L., Zubkov, T., Goralski, E.G., Walck, S.D. & Yates, J.T. Jr. 2004. Photochemical activity of nitrogen-doped rutile  $\text{TiO}_2$ (110) in visible light. *J. Phys. Chem. B* 108(19): 6004-6008.
- Fische, T.H. & Almlöf, J. 1992. General methods for geometry and wave function optimization. *J. Phys. Chem.* 96: 9768-9774.
- Fox, H., Newman, K.E., Schneider, W.F. & Corecelli, S.A. 2010. Bulk and surface properties of rutile  $\text{TiO}_2$  from self-consistent-charge density functional tight binding. *J. Chem. Theory Comput.* 6: 499-507.
- Fujishima, A. & Honda, K. 1972. Electrochemical photolysis of water at a semiconductor electrode. *Nature* 238(5358): 37-38.
- Gole, J.L., Stout, J.D., Burda, C., Lou, Y. & Chen, X. 2004. Highly efficient formation of visible light tunable  $\text{TiO}_{2-x}\text{N}_x$  photocatalysts and their transformation at the nanoscale. *J. Phys. Chem. B* 108(4): 1230-1240.
- Griffin, G.L. & Siefering, K.L. 1990. Growth kinetics of CVD  $\text{TiO}_2$ : Influence of carrier gas. *J. Electrochem. Soc.* 137(4): 1206-1208.
- Irie, H., Watanabe, Y. & Lindquist, S-E. 2003. Nitrogen-concentration dependence on photocatalytic activity of  $\text{TiO}_{2-x}$  powders. *J. Phys. Chem. B* 107(23): 5483-5486.
- Islam, M.M., Bredow, T. & Gerson, A. 2007. Electronic properties of oxygen-deficient and aluminum-doped rutile  $\text{TiO}_2$  from first principles. *Phys. Rev. B* 76(4): 045217.
- Iuga, M., Steinle-Neumann, G. & Meinhardt, J. 2007. *Ab-initio* simulation of elastic constants for some ceramic materials. *Eur. Phys. J. B* 58: 127-133.
- Janisch, R., Gopal, P. & Spaldin, N.A. 2005. Transition metal-doped  $\text{TiO}_2$  and  $\text{ZnO}$ -present status of the field. *J. Phys.: Condens. Matter* 17(27): R657.
- Khan, S.U.M., Al-Shahry, M. & Ingler, W.B. Jr. 2002. Efficient photochemical water splitting by a chemically modified n- $\text{TiO}_2$ . *Science* 297(5590): 2243-2245.
- Labat, F., Baranek, P., Domain, C., Minot, C. & Adamo, C. 2007. Density functional theory analysis of the structural and electronic properties of  $\text{TiO}_2$  rutile and anatase polytypes: Performances of different exchange-correlation functional. *J. Chem. Phys.* 126(15): 154703.
- Lazzeri, M., Vittadini, A. & Selloni, A. 2001. Structure and energetics of stoichiometric  $\text{TiO}_2$  anatase surfaces. *Phys. Rev. B* 63(15): 155409.
- Lin, Zh., Orlov, A., Lambert, R.M. & Payne, M.C. 2005. New insights into the origin of visible light photocatalytic activity of nitrogen-doped and oxygen-deficient anatase  $\text{TiO}_2$ . *J. Phys. Chem. B* 109(44): 20948-20952.
- Lindgren, T., Mwabora, J.M., Avendano, E., Jansson, J., Hoel, A., Granqvist, C-G. & Lindquist, S-E. 2003. Photoelectrochemical and optical properties of nitrogen doped titanium dioxide films prepared by reactive DC magnetron sputtering. *J. Phys. Chem. B* 107(24): 5709-5716.
- Liu, Y., Ni, L., Ren, Z., Xu, G., Song, C. & Han, G. 2009. Negative pressure induced ferroelectric phase transition in rutile  $\text{TiO}_2$ . *J. Phys.: Condens. Matter* 21(27): 275901.
- Ma, X.G., Liang, P., Miao, L., Bei, S.W., Zhang, C.K., Xu, L. & Jiang, J.J. 2009. Pressure-induced phase transition and elastic properties of  $\text{TiO}_2$  polymorphs. *Phys. Status Solidi B* 246(9): 2132-2139.
- Mattioli, G., Filippone, F., Alippi, P. & Bonapasta, A.A. 2008. *Ab initio* study of the electronic states induced by oxygen vacancies in rutile and anatase  $\text{TiO}_2$ . *Phys. Rev. B* 78(24): 241201.
- Monkhorst, H.J. & Pack, J.D. 1976. Special points for Brillouin-zone integrations. *Phys. Rev. B* 13: 5188-5192.
- Murnaghan, F.D. 1944. The compressibility of media under extreme pressures. *Proc. Natl. Acad. Sci. USA* 30(9): 244-247.
- Nakamura, R., Tanaka, T. & Nakato, Y. 2004. Mechanism for visible light responses in anodic photocurrents at n-doped  $\text{TiO}_2$  film electrodes. *J. Phys. Chem. B* 108(30): 10617-10620.
- Pascual, J., Camassel, J. & Mathieu, H. 1978. Fine structure in the intrinsic absorption edge of  $\text{TiO}_2$ . *Phys. Rev. B* 18(10): 5606-5614.

- Perdew, J.P., Burke, K. & Ernzerhof, M. 1996. Generalized gradient approximation made simple. *Phys. Rev. Lett.* 77: 3865-3868.
- Persson, C. & da Silva, A.F. 2005. Strong polaronic effects on rutile TiO<sub>2</sub> electronic band edges. *Appl. Phys. Letts.* 86(23): 231912.
- Sakthivel, S. & Kisch, H. 2003. Photocatalytic and photoelectrochemical properties of nitrogen-doped titanium dioxide. *ChemPhysChem* 4(5): 487-490.
- Segall, M.D., Lindan, P., Probet, M.J., Pickard, C.J., Hasnip, P.J., Clark, S.J. & Payne, M.C. 2002. First-principles simulation: Ideas, illustrations and the CASTEP code. *J. Phys. Condens. Matter* 14: 2717-2744.
- Shi, H., Luo, W., Johansson, B. & Ahuja, R. 2009. Electronic and elastic properties of CaF<sub>2</sub> under high pressure from *ab initio* calculations. *J. Phys. Condens. Matter* 21(41): 415501.
- Shirley, R., Kraft, M. & Inderwildi, O.R. 2010. Electronic and optical properties of aluminium-doped anatase and rutile TiO<sub>2</sub> from *ab initio* calculations. *Phys. Rev. B* 81: 075111.
- Swamy, V. & Muddle, B.C. 2007. Ultrastiff cubic TiO<sub>2</sub> identified via first-principles calculations. *Phys. Rev. Lett.* 98(3): 035502.
- Tang, H., Berger, H., Schmid, P.E., Levy, F. & Burri, G. 1993. Photoluminescence in TiO<sub>2</sub> anatase single crystals. *Solid State Commun.* 87(9): 847-850.
- Tariq Mahmood, Chuanbao Cao, Waheed S. Khan, Zahid Usman, Faheem K. Butt & Sajad Hussain. 2012. Electronic, elastic, optical properties of rutile TiO<sub>2</sub> under pressure: A DFT study. *Physica B: Condensed Matter* 207: 958-965.
- Thilagam, A., Simpson, D.J. & Gerson, A.R. 2011. A first-principles study of the dielectric properties of TiO<sub>2</sub> polymorphs. *J. Phys. Condens. Matter* 23(2): 025901.
- Varghese, O.K. & Grimes, C.A. 2003. Metal oxide nanoarchitectures for environmental sensing. *J. Nanosci. Nanotech.* 3(4): 277-293.
- Wu, J.M. & Chen, C.J. 1990. Effect of powder characteristics on microstructures and dielectric properties of (Ba,Nb)-doped titania ceramics. *J. Am. Ceram. Soc.* 73(2): 420-424.
- Yahya Al-Khatibeh, Kanani K.M. Lee & Boris Kiefer. 2009. High-pressure behavior of TiO<sub>2</sub> as determined by experiment and theory. *Phys. Rev. B* 79(13): 134114.
- Yin, W-J., Chen, S., Yang, J-H., Gong, X-G., Yan, Y. & Wei, S-H. 2010. Effective bandgap narrowing of anatase TiO<sub>2</sub> by strain along a soft crystal direction. *Appl. Phys. Lett.* 96(22): 221901.
- Zhao, W., Ma, W., Chen, Ch., Zhao, J. & Shuai, Zh. 2004. Efficient degradation of toxic organic pollutants with Ni<sub>2</sub>O<sub>3</sub>/TiO<sub>2-x</sub>B<sub>x</sub> under visible irradiation. *J. Am. Chem. Soc.* 126(15): 4782-4783.
- Zhou, X-F., Dong, X., Qian, G-R., Zhang, L., Tian, Y. & Wang, H-T. 2010. Unusual compression behavior of TiO<sub>2</sub> polymorphs from first principles. *Phys. Rev. B* 82(6): 060102(R).
- Tariq Mahmood\*, Chuanbao Cao & M.A. Kamran  
School of Materials Science and Engineering  
Beijing Institute of Technology  
Beijing-100081  
P.R. China
- Tariq Mahmood\*. Maqsood Ahmed, Abrar Ahmed Zafar  
& Talab Husain  
Centre for High Energy Physics  
University of the Punjab  
Lahore-54590  
Pakistan
- Rashid Ahmed & M.A. Saeed  
Physics Department  
Faculty of Science  
Universiti Teknologi Malaysia  
UTM Skudai, 81310 Johor  
Malaysia
- \*Corresponding author; email: tariq\_mahmood78@hotmail.com
- Received: 7 January 2012  
Accepted: 21 May 2012